PAPER

Calculation of deformed double-folding potentials in the context of the generalized rotation-vibration model

To cite this article: D F Morales Botero et al 2014 J. Phys. G: Nucl. Part. Phys. 41 055114

View the article online for updates and enhancements.

You may also like

- Analysis of fusion dynamics of colliding systems involving stable, loosely bound and halo nuclei
 Manjeet Singh Gautam
- Transition densities in the context of the generalized rotation-vibration model

 D F Morales Botero, L C Chamon and B V Carlson
- Folding-type coupling potentials in the context of the generalized rotation-vibration model

Calculation of deformed double-folding potentials in the context of the generalized rotation-vibration model

D F Morales Botero¹, L C Chamon¹ and B V Carlson²

- ¹ Departamento de Física Nuclear, Instituto de Física da Universidade de São Paulo, Caixa Postal 66318, 05315-970, São Paulo, SP, Brazil
- ² Departamento de Física, Instituto Tecnológico de Aeronáutica, São José dos Campos, SP, Brazil

E-mail: lchamon@if.usp.br

Received 15 January 2014, revised 7 March 2014 Accepted for publication 7 March 2014 Published 2 April 2014

Abstract

We present a procedure to calculate quite accurately double-folding potentials involving deformed densities. The calculations are performed in the context of the generalized rotation-vibration model, which is a general approach to describe rotations and vibrations of nuclear densities for heavy nuclei. The present method is appropriate for obtaining the coupling potentials intended for future applications in coupled-channel calculations. We compare our results with those obtained from other models usually assumed in coupled-channel analyses.

Keywords: double-folding potential, coupled-channel models, optical models (Some figures may appear in colour only in the online journal)

1. Introduction

There are many phenomena of nuclear structure that can be understood by considering the collective movement of the nucleons in the nucleus. The idea behind several collective models implies treating the nucleus as an incompressible drop that can be deformed. There are two extreme approaches in this context: in the rotational model (RM) the nucleus has a fixed deformed shape, while in the vibrational model (VM) it can vibrate around the spherical shape. Many nuclei present low-lying level schemes quite similar to those predicted by the RM or VM. Eisenberg and Greiner proposed the rotation-vibration model [1], in which small amplitudes of vibration around an average deformation are allowed. The case where there is no restriction between the amplitude of vibration and the average deformation values was

recently proposed in [2]. We refer to this approach as the generalized rotation-vibration model (GRVM). The scope of the GRVM includes the cases of the quadrupole and octupole deformations for even-even nuclei. It also takes into account the effects of the diffuseness of the nuclear densities, which is usually neglected in other models.

Due to their internal structure, the collision between heavy-ions results in many different processes, such as elastic and inelastic scattering, transfer reactions and nuclear fusion. A fundamental approach to this kind of problem is through coupled-channel (CC) calculations (see e.g. [3, 4]), where a few channels are explicitly considered in the solution of the corresponding coupled equations, while the effect of the others should be simulated by the optical potential. Many works have demonstrated that the couplings have an important effect on the calculation of cross sections for several processes (for review see e.g. [4–10]). In particular, it was discovered in the late 1970s [11–13] and confirmed in many works [4-10] that, at sub-Coulomb energy region, the couplings can represent an enhancement of several orders of magnitude of the fusion cross sections in comparison with results obtained from the unidimensional barrier penetration model. For most of systems, this enhancement is associated with the inelastic couplings related to the states of the quadrupole and octupole bands [14–16]. As already commented, these bands are described in the context of the GRVM. On the other hand, CC calculations have not accounted for the experimental fusion cross sections at extreme sub-barrier energies (e.g. [17]). Furthermore, a lack of consistence between potentials assumed to describe the fusion and elastic scattering processes has been found (e.g. [18]). It was suggested in [19] that the disagreement between the data and theoretical results could be related to some approximations and/or modeling commonly assumed in CC calculations, which may result in inaccurate cross sections, especially in the case of systems involving highly deformed nuclei. Taking this case into account, a method to obtain deformed potentials with a high degree of precision would be of importance to test the accuracy of the results currently obtained from the usual numerical CC calculations. This is, indeed, the main goal of the present work.

The calculation of double-folding potentials involves a six-dimensional integral that, in the case of spherical densities, can be easily performed through the Fourier transform method [20]. In the case of deformed densities, the six-dimensional integral can also be calculated without any approximation, directly from numerical integration as well as through the Fourier transform method, although both procedures require considerable computation time. Even so, these methods are not appropriate for application in CC calculations. In fact, the corresponding coupling potentials involve the folding of the deformed potential with the wave-functions that describe the states of the nucleus. In general, these wave-functions depend on several coordinates (of deformation) and, therefore, the calculation of coupling potentials generally involve multi-dimensional integrals that, in practice, cannot be solved numerically. Thus, methods to solve these multi-dimensional integrals analytically, at least in part, are very important to practical applications in CC calculations. A possible form to obtain this result is to express the deformed potential as an explicit function of the deformations, as performed, for example, in [21, 22] for the case of the Coulomb interaction. We point out that, due to the corresponding simplicity for calculation, coupling-potentials usually assumed for the Coulomb interaction in CC calculations arise from models where the sharp cutoff shape (vanishing diffuseness) is adopted for the charge distributions (see e.g. [7, 21, 23]).

In the present paper, we present a general procedure to calculate quite accurately double-folding potentials involving deformed densities. The method is a generalization of that reported in [21, 22] and is based on the expansion of the nuclear densities up to second order in the deformation. In the present work, we apply the procedure to the calculation of both, the nuclear and Coulomb, interactions in the particular context of the GRVM, but the method can also

be easily applied to different models. With the purpose of testing the corresponding accuracy, we compare our results with those from common approximations usually assumed in CC calculations, and also with exact results from the numerical calculation of the six-dimensional integral. We also study the effect of assuming a finite value for the nuclear diffuseness on the deformed Coulomb potential.

In section 2 we present a brief review of nuclear densities and of the GRVM. The methods to calculate deformed potentials without approximation are described in section 3. Section 4 presents models usually assumed for the Coulomb and nuclear potentials, while section 5 describes the present method of calculation. In section 6, we discuss the results of the different approximations in the case of a system involving quite deformed nuclei. Section 7 contains our main conclusions.

2. Nuclear densities and GRVM

In this section we present a brief description of nuclear distributions in the context of the GRVM [2]. In a totally general basis, the nuclear density can be described, in a frame whose origin coincides with the center of mass of the nucleus, by a function $\rho(\vec{r})$, where \vec{r} is the position vector of a point in space in the direction $\Omega_r = (\theta, \phi)$. In the present work, we only consider deformed densities that can be expressed as a function of r and Δ , where Δ is the deformation in the direction (θ, ϕ) , which can be expanded in multipoles:

$$\rho(\vec{r}) = \rho(r, \Delta),\tag{1}$$

$$\Delta(\theta, \phi) = \sum_{\lambda=0}^{\infty} \sum_{\mu=-\lambda}^{\lambda} \alpha_{\lambda\mu}^* Y_{\lambda\mu}(\theta, \phi). \tag{2}$$

In (2), $Y_{\lambda\mu}$ are the spherical harmonics and $\alpha_{\lambda\mu}$ are the coordinates of deformation. Since the deformation must be a real number, one obtains:

$$\alpha_{\lambda\mu} = (-1)^{\mu} \alpha_{\lambda-\mu}^*. \tag{3}$$

If the frame of reference is rotated by a set of Euler angles $(\theta_1, \theta_2, \theta_3)$, the coordinates of deformation are transformed as:

$$\alpha_{\lambda\mu} = \sum_{\mu'} D_{\mu\mu'}^{\lambda*}(\theta_1, \theta_2, \theta_3) a_{\lambda\mu'},\tag{4}$$

where $D_{\mu\mu'}^{\lambda}$ are the Wigner rotation functions (we follow here the conventions of [1, 2]).

The calculations of the Coulomb and nuclear potentials involve, respectively, the charge and matter distributions. These distributions should be normalized as follows:

$$\int \rho(r, \Delta) \, d\vec{r} = A \text{ (matter) or } Z \text{ (charge)}$$
 (5)

where A and Z are the numbers of mass and protons of the nucleus, respectively. We define the spherical density $\rho_0(r)$ associated to the deformed one through:

$$\rho_0(r) = \rho(r, 0). \tag{6}$$

In this context, the nuclear incompressibility can be expressed by the invariance of the volume relative to the deformation, i.e.:

$$\int \rho(r, \Delta) \, d\vec{r} = 4\pi \int \rho_0(r) \, r^2 \, dr. \tag{7}$$

Since the center of mass must coincide with the origin of the frame of reference, we have:

$$\int \rho(r, \Delta) \, \vec{r} \, \mathrm{d}\vec{r} = 0. \tag{8}$$

(7) and (8) represent links among the coordinates of deformation. Through them, the monopole and dipole (α_{00} and $\alpha_{1\mu}$) parameters can be considered as functions of the coordinates of the higher orders.

Within the GRVM, the Fermi distribution is assumed to represent the deformed shape of the nucleus, by expanding the nuclear radius in multipoles:

$$\rho(r,\Delta) = \frac{\epsilon_0}{1 + \exp\left\{ [r - R_0(1+\Delta)]/a \right\}},\tag{9}$$

where ϵ_0 is the normalization constant and a is the nuclear diffuseness. Furthermore, only terms up to octupole are considered in the expansion (2). The quadrupole and octupole modes are totally independent. The corresponding intrinsic frames of reference are defined as those where the coordinates of deformation can be written as:

$$a_{20} = \beta_2 \cos \gamma; \quad a_{21} = a_{2-1} = 0; \quad a_{22} = a_{2-2} = \frac{\beta_2}{\sqrt{2}} \sin \gamma,$$
 (10)

$$a_{30} = \beta_3; \quad a_{3\mu} = 0 (\mu \neq 0).$$
 (11)

Since we have considered only terms up to the octupole order in (2), a fixed shape of a deformed nucleus can be expressed, in the laboratory frame of reference, through the $16 \alpha_{\lambda\mu}$ complex coordinates. On the other hand, these coordinates are related by equations (3) to (8), (10) and (11), and, therefore, they are functions of only 9 (real) coordinates: β_2 , γ , β_3 and the two sets of Euler angles for $\lambda=2$ and 3.

Considering only contributions to second order, as well as an approximation to the Fermi distribution [24], (7) and (8) result in [2]:

$$\alpha_{00} \approx -\frac{1}{\sqrt{4\pi}} \left(\frac{\beta_2^2 + \beta_3^2}{1 + \frac{77a^2}{24R_0^2}} \right), \tag{12}$$

$$\alpha_{10} \approx -\sqrt{\frac{27}{140\pi}} \frac{\left(1 + \frac{77a^2}{24R_0^2}\right)}{\left(1 + \frac{77a^2}{8R_0^2} + \frac{11a^3}{24R_0^3}\right)} [3\alpha_{20}\alpha_{30} + \sqrt{8}(\alpha_{21}\alpha_{31}^* + \alpha_{21}^*\alpha_{31}) + \sqrt{5}(\alpha_{22}\alpha_{32}^* + \alpha_{22}^*\alpha_{32})], \tag{13}$$

$$\alpha_{11} \approx \sqrt{\frac{27}{140\pi}} \frac{\left(1 + \frac{77a^2}{24R_0^2}\right)}{\left(1 + \frac{77a^2}{8R_0^2} + \frac{11a^3}{24R_0^3}\right)} (\sqrt{3}\alpha_{30}\alpha_{21} - \sqrt{6}\alpha_{20}\alpha_{31} + \alpha_{22}\alpha_{31}^* - \sqrt{10}\alpha_{21}^*\alpha_{32} - \sqrt{15}\alpha_{22}^*\alpha_{33}).$$

$$(14)$$

Following the systematics reported in [2], the diffuseness values of the densities are taken to be:

$$a = 0.50 + 0.00018A \text{ (fm)}.$$
 (15)

The radius of the spherical nucleus is obtained for charge distributions from:

$$R_0 = 1.67Z^{1/3} + 0.57(N^{1/3} - Z^{1/3}) - 0.97(\text{fm}),$$
 (16)

where N is the number of neutrons of the nucleus. For matter distributions we have:

$$R_0 = \frac{N \times R_{\text{neutron}} + Z \times R_{\text{proton}}}{A},\tag{17}$$

where R_{proton} is the R_0 of the charge distribution and R_{neutron} is obtained from (16) by exchanging N and Z. The ϵ_0 parameter can be found from the normalization of the densities (5).

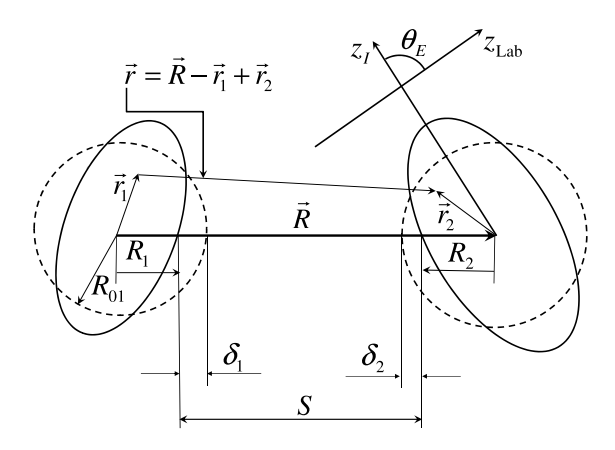


Figure 1. Schematic representation of the collision between two nuclei. The solid and dashed lines represent the deformed and spherical radii of the nuclei, respectively. Z_{Lab} and Z_I represent the laboratory frame of reference and the intrinsic frame of nucleus 2. In this case, θ_E represents the set of Euler angles for nucleus 2. \vec{R} connects the centers of mass of both nuclei. The figure indicates the radius of the associated spherical nucleus 1 (R_{01}) and the radii of the two deformed nuclei in the direction of \vec{R} (R_1 and R_2). S is the distance between surfaces in the direction of \vec{R} and δ_1 and δ_2 are the differences between deformed and spherical radii in this same direction.

3. Exact methods of calculation of double-folding potentials

Figure 1 presents a scheme of a nuclear collision. The solid and dashed curves represent the radii of the deformed and associated spherical nuclei, respectively. Z_{Lab} and Z_I represent the laboratory frame of reference and the intrinsic frame of nucleus 2, and, thus, θ_E represents the set of Euler angles for nucleus 2. \vec{R} is the vector that connects the centers of mass of both nuclei. The double-folding potential between these nuclei can be written as [20]:

$$V(\vec{R}) = \int \rho_1(\vec{r}_1)\rho_2(\vec{r}_2)u(\vec{R} - \vec{r}_1 + \vec{r}_2) \,\mathrm{d}\vec{r}_1 \,\mathrm{d}\vec{r}_2. \tag{18}$$

For the Coulomb interaction: $u(\vec{r}) = e^2/r$. In the case of the nuclear potential, $u(\vec{r})$ represents the effective nucleon–nucleon interaction. In our present calculations, we assume the São Paulo potential [24] where, for low energies, we have $u(\vec{r}) = V_0 \, \delta(\vec{r})$, with $V_0 = -456$ MeV fm³. Due to the Dirac delta function, in this case we can rewrite (18) as:

$$V(\vec{R}) = V_0 \int \rho_1(\vec{r}_1) \rho_2(\vec{r}_1 - \vec{R}) \, d\vec{r}_1. \tag{19}$$

We point out, however, that the methods presented in this work can be easily adapted to other models of the nuclear interaction.

The Fourier transform of a function $u(\vec{r})$ and its inverse are given by:

$$\tilde{u}(\vec{k}) = \int u(\vec{r}) \,\mathrm{e}^{\mathrm{i}\vec{k}\cdot\vec{r}} \,\mathrm{d}\vec{r},\tag{20}$$

$$u(\vec{r}) = \frac{1}{8\pi^3} \int \tilde{u}(\vec{k}) e^{-i\vec{k}\cdot\vec{r}} d\vec{k}. \tag{21}$$

Thus, (18) can be written as:

$$V(\vec{R}) = \frac{1}{8\pi^3} \int \tilde{u}(\vec{k}) \rho_1(\vec{r}_1) \rho_2(\vec{r}_2) e^{-i\vec{k}\cdot(\vec{R}+\vec{r}_2-\vec{r}_1)} d\vec{k} d\vec{r}_1 d\vec{r}_2$$
 (22)

where

$$\tilde{u}(\vec{k}) = 4\pi e^2/k^2$$
 Coulomb potential, (23)

$$\tilde{u}(\vec{k}) = V_0$$
 São Paulo potential. (24)

Following [21], we use the plane-wave expansion:

$$e^{i\vec{k}\cdot\vec{r}} = 4\pi \sum_{\lambda\mu} i^{\lambda} j_{\lambda}(kr) Y_{\lambda\mu}^{*}(\Omega_{k}) Y_{\lambda\mu}(\Omega_{r}),$$

$$e^{-i\vec{k}\cdot\vec{r}} = 4\pi \sum_{\lambda\mu} i^{-\lambda} j_{\lambda}(kr) Y_{\lambda\mu}(\Omega_{k}) Y_{\lambda\mu}^{*}(\Omega_{r}),$$
(25)

where $j_{\lambda}(kr)$ are the spherical Bessel functions. According to (23) and (24), $\tilde{u}(\vec{k})$ does not in fact depend on the direction Ω_k in the cases of the Coulomb and São Paulo potentials. Considering this fact as well as (25), (22) can be rewritten as:

$$V(\vec{R}) = \sum_{\lambda\mu} V_{\lambda\mu}(R) Y_{\lambda\mu}^*(\Omega_R) = \sum_{\lambda\mu} V_{\lambda\mu}^*(R) Y_{\lambda\mu}(\Omega_R), \tag{26}$$

$$V_{\lambda\mu}(R) = 8 \sum_{\lambda_1\mu_1} \left\{ \sum_{\lambda_2\mu_2} i^{\lambda_1 - \lambda_2 - \lambda} \left[\int \tilde{v}(k) j_{\lambda}(kR) M_{\lambda_1\mu_1}^{(1)}(k) M_{\lambda_2\mu_2}^{(2)}(k) k^2 dk \right] \right. \\ \left. \times \left[\int Y_{\lambda\mu}(\Omega_k) Y_{\lambda_1\mu_1}^*(\Omega_k) Y_{\lambda_2\mu_2}^*(\Omega_k) d\Omega_k \right] \right\}$$
(27)

$$M_{\lambda\mu}^{(i)}(k) = \int \rho_i(\vec{r}) j_{\lambda}(kr) Y_{\lambda\mu}(\Omega_r) d\vec{r}.$$
 (28)

The integral of the three spherical harmonics of (27) can be expressed through Clebsch–Gordan coefficients (again we follow the conventions of [1]):

$$\int Y_{\lambda\mu}(\Omega)Y_{\lambda_1\mu_1}^*(\Omega)Y_{\lambda_2\mu_2}^*(\Omega)\,\mathrm{d}\Omega = \sqrt{\frac{(2\lambda_1+1)(2\lambda_2+1)}{4\pi(2\lambda+1)}}\,C_{\mu_1\mu_2\mu}^{\lambda_1\lambda_2\lambda}\,C_{0\ 0\ 0}^{\lambda_1\lambda_2\lambda},\tag{29}$$

where $C_{\mu_1\mu_2\mu}^{\lambda_1\lambda_2\lambda}$ is the Clebsch–Gordan coefficient that couples the λ_1 and λ_2 angular momenta producing a total λ angular momentum. Thus, the sum of (27) is limited to the terms with $\mu_2 = \mu - \mu_1$ and $|\lambda_1 - \lambda| \leq \lambda_2 \leq \lambda_1 + \lambda$. If the Z_{Lab} axis of the laboratory frame of reference coincides with \vec{R} , the nonvanishing terms of (26) are only those with $\mu = 0$ and, for these, $Y_{\lambda 0}(\Omega_R) = \sqrt{(2\lambda + 1)/4\pi}$.

For spherical densities, all $M_{\lambda\mu}$ of (28) are equal to zero, except that with $\lambda = \mu = 0$ which is given by $M_{00}(k) = \sqrt{4\pi} \hat{\rho}_0(k)$, where:

$$\hat{\rho}_0(k) = \int j_0(kr) \, \rho_0(r) \, r^2 \, \mathrm{d}r. \tag{30}$$

The six-dimensional integral of (18) can be calculated without approximation, directly by numerical integration as well as by making use of the Fourier transform method through (26) to (28). However, these procedures are not appropriated for calculating coupling potentials because the latter involve the folding of the deformed potential with the wave-functions of the nuclear states. For instance, consider the case of two deformed nuclei, each with 9 coordinates of deformation (β_2 , γ , β_3 and the two sets of Euler angles for $\lambda = 2$ and 3). This would imply the calculation of the six-dimensional integral, represented by (18), folded into a 18-dimensional integral involving the deformation coordinates, resulting in an integral of dimension 24! Of course, such an integral cannot be calculated using common numerical procedures and, thus, methods to solve it, at least partially, within an analytical form are indispensable.

4. Common approximations to calculate the deformed potential

There are several computer programs that have been successfully used in the CC data analyses of many works, such as CCFULL [25], FRESCO [26], ECIS [27], etc. Some of them have options of reading the diagonal and coupling potentials from external files. In this context, the CC calculations are quite general and any model for the couplings can be implemented. Nevertheless, in this case the user has the responsibility of calculating these potentials within that hypothetical model. For this reason, most works performed with those codes assume options in which the potentials have standard shapes like the Woods-Saxon, Gaussian, etc. In the case of the inelastic couplings, the deformation of the densities, which results in the deformed potentials, is not taken into account through the double-folding procedure, and commonly the coupling potentials are obtained from some procedure involving the bare diagonal interaction. Thus, before proceeding with the description of the present method to calculate deformed potentials, we first present other models often assumed in CC calculations, with the purpose of comparing the corresponding results with those of the present model.

Hereafter, we indicate the double-folding potential obtained with the associated spherical densities (undeformed potential) by $V_{\rm U}(R)$, and that obtained with the deformed densities (deformed potential) as $V_D(\vec{R})$. The difference between these two potentials is referred as the correction potential $V_{\text{Cor}}(\vec{R}) = V_{\text{D}}(\vec{R}) - V_{\text{U}}(R)$. We focus our attention on V_{Cor} since the effects of the deformation are contained there.

Due to the short-range of the nuclear interaction, the nuclear potential should be reasonably well described by a function of the distance between the surfaces of the nuclei, represented by S in figure 1. On the other hand, this distance can be written in terms of the radii of the deformed and spherical nuclei as:

$$S = R - R_1 - R_2 = R - R_{01} - R_{02} - \delta, (31)$$

where $\delta = \delta_1 + \delta_2$ (see figure 1). Therefore, the nuclear potential can be represented by a

function of argument
$$R - \delta$$
, $V_{\rm D}(R - \delta)$. For small deformation values, it can be expanded as:
$$V_{\rm D}(\vec{R}) \approx V_{\rm U}(R) + \sum_n \frac{1}{n!} \left. \frac{\partial^n V_{\rm D}}{\partial \delta^n} \right|_{\delta=0} \delta^n \approx V_{\rm U}(R) + \sum_n \frac{(-1)^n}{n!} \frac{d^n V_{\rm U}}{dR^n} \delta^n. \quad (32)$$

With this, we can write the difference between deformed and undeformed nuclear potentials as:

$$V_{\text{Cor}}(\vec{R}) \approx \sum_{n} \frac{(-1)^n}{n!} \frac{d^n V_{\text{U}}}{dR^n} \, \delta^n.$$
 (33)

When the Z_{Lab} axis of the laboratory frame of reference coincides with the vector \vec{R} , we can write the deformations of the two nuclei as:

$$\delta_1 = R_{01} \times \sum_{\lambda=0}^{3} \sum_{\mu=-\lambda}^{\lambda} \alpha_{\lambda\mu 1}^* Y_{\lambda\mu}(\theta = 0, \phi) = \frac{R_{01}}{2\sqrt{\pi}} \times \sum_{\lambda=0}^{3} \sqrt{2\lambda + 1} \alpha_{\lambda 0 1}, \tag{34}$$

$$\delta_2 = R_{02} \times \sum_{\lambda=0}^{3} \sum_{\mu=-\lambda}^{\lambda} \alpha_{\lambda\mu 2}^* Y_{\lambda\mu}(\theta = \pi, \phi) = \frac{R_{02}}{2\sqrt{\pi}} \times \sum_{\lambda=0}^{3} (-1)^{\lambda} \sqrt{2\lambda + 1} \, \alpha_{\lambda 0 2}.$$
 (35)

Observe that the $\alpha_{\lambda\mu}$ of these equations are first order terms for $\lambda=2$ and 3, and correspond to second order terms for $\lambda = 0$ and 1. This should be taken into account when calculating the potential in first or second order through (32). We point out that the calculation of the deformed potential from (33) does not involve the double-folding calculation with the deformed densities, since it depends only on the derivatives of the undeformed (bare) potential. Due to its simplicity, this approximation has been widely applied in usual CC calculations.

In the case of the Coulomb interaction, it is usual to expand the potential in multipoles, where the sharp cutoff shape is assumed to describe the densities, with some model to correct the shape of the potential in the region where there is superposition of densities (see e.g. [21]). For instance, within the uniform charge model we have, to first order:

$$V_{\text{Cor}}(\vec{R}) \approx \frac{Z_1 Z_2 e^2}{2\sqrt{\pi}} \left\{ \sum_{\lambda=2}^{3} F_{\lambda}(R) \left[\alpha_{\lambda 01} \left(\frac{R_{01}}{R_C} \right)^2 + (-1)^{\lambda} \alpha_{\lambda 02} \left(\frac{R_{02}}{R_C} \right)^2 \right] \right\}, \tag{36}$$

$$F_{\lambda}(R) = \frac{3}{\sqrt{2\lambda + 1}} \begin{cases} R_C^{\lambda} / R^{\lambda + 1} & \text{for } R > R_C \\ R^{\lambda} / R_C^{\lambda + 1} & \text{for } R \leqslant R_C \end{cases}$$
(37)

where $R_C = R_{01} + R_{02}$. In this expression, it is assumed that the laboratory Z_{LAB} axis is in the direction of \vec{R} .

5. Calculating the potential in the context of the GRVM

We turn now to the present method of calculation of deformed potentials. We expand the densities of (1) to second order in the deformation:

$$\rho(\vec{r}) \approx \rho_0(r) + (\Delta_1 + \Delta_2) \left. \frac{\partial \rho}{\partial \Delta} \right|_{\Delta = 0} + \left. \frac{\Delta_3}{2} \frac{\partial^2 \rho}{\partial \Delta^2} \right|_{\Delta = 0}, \tag{38}$$

$$\Delta_1 = \sum_{\lambda=2}^3 \sum_{\mu=-\lambda}^{\lambda} \alpha_{\lambda\mu}^* Y_{\lambda\mu}(\Omega_r), \tag{39}$$

$$\Delta_2 = \sum_{\lambda=0}^{1} \sum_{\mu=-\lambda}^{\lambda} \alpha_{\lambda\mu}^* Y_{\lambda\mu}(\Omega_r), \tag{40}$$

$$\Delta_3 = \sum_{\lambda=2}^3 \sum_{\mu=-\lambda}^{\lambda} \sum_{\lambda'=2}^3 \sum_{\mu'=-\lambda'}^{\lambda'} \alpha_{\lambda\mu}^* \alpha_{\lambda'\mu'}^* Y_{\lambda\mu}(\Omega_r) Y_{\lambda'\mu'}(\Omega_r). \tag{41}$$

In these equations, Δ_1 is a first order term in the deformations, while Δ_2 and Δ_3 are terms of second order. Substituting these equations into (28) and making use of the properties of the spherical harmonics, we obtain:

$$M_{\lambda\mu}(k) = \delta_{\lambda 0} I^{(0)}(k) + \alpha_{\lambda\mu} I_{\lambda}^{(1)}(k) + (-1)^{\mu} I_{\lambda}^{(2)}(k)$$

$$\times \sum_{\lambda'\mu'} \sum_{\lambda'''\mu''} \alpha_{\lambda''\mu''}^* \sqrt{\frac{(2\lambda'+1)(2\lambda''+1)}{4\pi (2\lambda+1)}} C_{\mu'\mu''-\mu}^{\lambda'\lambda''\lambda} C_{0\ 0\ 0}^{\lambda'\lambda''\lambda}, \tag{42}$$

$$I^{(0)}(k) = \sqrt{4\pi} \,\,\hat{\rho}_0(k),\tag{43}$$

$$I_{\lambda}^{(1)}(k) = \int j_{\lambda}(kr) \left. \frac{\partial \rho}{\partial \Delta} \right|_{\Delta=0} r^2 \, \mathrm{d}r, \tag{44}$$

$$I_{\lambda}^{(2)}(k) = \frac{1}{2} \int j_{\lambda}(kr) \left. \frac{\partial^2 \rho}{\partial \Delta^2} \right|_{\Delta = 0} r^2 \, \mathrm{d}r. \tag{45}$$

The sums in (42) are performed only over $\lambda'=2$, 3 and $\lambda''=2$, 3. Thus, taking into account the properties of the Clebsch–Gordan coefficients in (42) and that $\alpha_{\lambda\mu}=0$ for $\lambda>3$, all $M_{\lambda\mu}(k)$ elements vanish for $\lambda>6$, and the sum in (28) is performed only up to $\lambda=12$.

In order to be consistent, since we have adopted (38) to describe the densities, this equation should also be used in expressions (7) and (8) that connect the deformation parameters. With this, we obtain:

$$\alpha_{00} = -\left(\frac{\beta_2^2 + \beta_3^2}{4\sqrt{\pi}}\right) \left[\frac{\int \frac{\partial^2 \rho}{\partial \Delta^2} \Big|_{\Delta=0} r^2 dr}{\int \frac{\partial \rho}{\partial \Delta} \Big|_{\Delta=0} r^2 dr}\right],\tag{46}$$

$$\alpha_{10} = -\sqrt{\frac{3}{140\pi}} \left[\frac{\int \frac{\partial^{2} \rho}{\partial \Delta^{2}} \Big|_{\Delta=0} r^{3} dr}{\int \frac{\partial \rho}{\partial \Delta} \Big|_{\Delta=0} r^{3} dr} \right] [3\alpha_{20}\alpha_{30} + \sqrt{8}(\alpha_{21}\alpha_{31}^{*} + \alpha_{21}^{*}\alpha_{31}) + \sqrt{5}(\alpha_{22}\alpha_{32}^{*} + \alpha_{22}^{*}\alpha_{32})], \tag{47}$$

$$\alpha_{11} = \sqrt{\frac{3}{140\pi}} \left[\frac{\int \frac{\partial^2 \rho}{\partial \Delta^2} \Big|_{\Delta=0} r^3 \, dr}{\int \frac{\partial \rho}{\partial \Delta} \Big|_{\Delta=0} r^3 \, dr} \right] (\sqrt{3} \, \alpha_{30} \alpha_{21} - \sqrt{6} \alpha_{20} \alpha_{31} + \alpha_{22} \alpha_{31}^* - \sqrt{10} \alpha_{21}^* \alpha_{32} - \sqrt{15} \alpha_{22}^* \alpha_{33}).$$

$$(48)$$

For heavy-ions the results of these equations are indeed similar to those of (12)–(14). Even so, (46)–(48) should be used when (38) is assumed to describe the densities.

Assuming now (9) as the explicit form for the density of the GRVM, we obtain:

$$\left. \frac{\partial \rho}{\partial \Delta} \right|_{\Delta=0} = \frac{\epsilon_0 R_0}{a} \frac{\exp\left(\frac{r - R_0}{a}\right)}{\left[1 + \exp\left(\frac{r - R_0}{a}\right)\right]^2},\tag{49}$$

$$\left. \frac{\partial^2 \rho}{\partial \Delta^2} \right|_{\Delta=0} = \frac{\epsilon_0 R_0^2}{a^2} \frac{\exp\left(\frac{r - R_0}{a}\right) \left[\exp\left(\frac{r - R_0}{a}\right) - 1\right]}{\left[1 + \exp\left(\frac{r - R_0}{a}\right)\right]^3}.$$
 (50)

The deformed potential can then be calculated with (26), (27), (29), (42) to (45), (49) and (50). In this case, the dependence of the potential on the deformations is explicit through (42). This form allows the calculation of coupling-potentials analytically, which is the goal of the present method. This is not the case of the exact calculation through (28), where the dependence of $M_{\lambda\mu}(k)$ on the coordinates of deformation is not explicit.

The method can easily be generalized to other models, in which the density can be expressed according to (1), just by considering the corresponding derivatives with respect to Δ , as performed above in the context of the GRVM. In the case of the Coulomb potential, as already commented, several approaches assume the sharp cutoff shape for the charge densities (see e.g. [21]). In [22], the effect of the finite diffuseness value was taken into account, but within a more restrict model than that presented here. Within the sharp cutoff approach, the Coulomb potential can also be calculated through (26), (27), (29) and (42), with:

$$I^{(0)}(k) = \frac{3Z}{\sqrt{4\pi}} \frac{j_1(kR_0)}{kR_0},\tag{51}$$

$$I_{\lambda}^{(1)}(k) = \frac{3Z}{4\pi} j_{\lambda}(kR_0), \tag{52}$$

$$I_{\lambda}^{(2)}(k) = \frac{3Z}{4\pi} \left[j_{\lambda}(kR_0) + \frac{kR_0}{2} \left. \frac{\partial j_{\lambda}(x)}{\partial x} \right|_{x=kR_0} \right].$$
 (53)

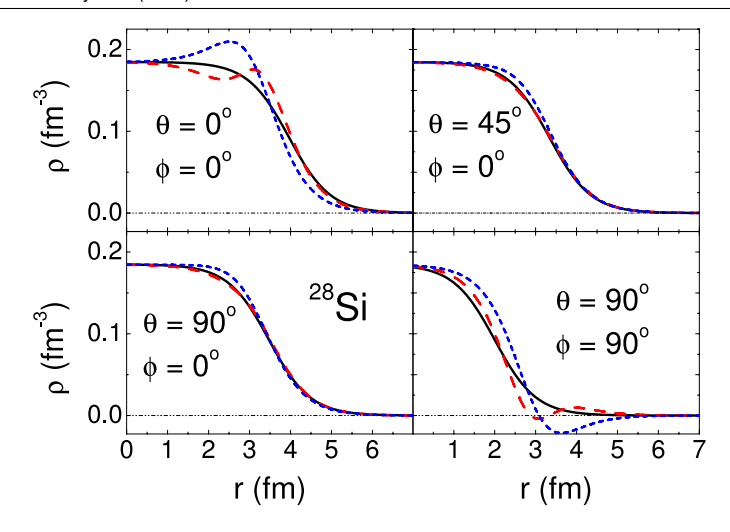


Figure 2. Matter density of the ²⁸Si nucleus for different spatial directions in the intrinsic frame of reference (for the quadrupole and octupole modes). The solid black lines correspond to the exact results of (9). The dotted blue and dashed red lines correspond to the results of (38), to first and second orders respectively.

Table 1. Average $(\bar{\beta}_2, \gamma_0 \text{ and } \bar{\beta}_3)$ and amplitude of vibration $(b_2 \text{ and } b_3)$ values for the quadrupole and octupole modes of the ²⁸Si and ¹⁵⁴Sm nuclei. The table also provides the β_2 , γ and β_3 values assumed in our calculations of deformed potentials.

Nucleus	$ar{eta}_2$	γ 0	b_2	$ar{eta}_3$	b_3	eta_2	γ	β_3
²⁸ Si ¹⁵⁴ Sm			0.15 0.056					0.24 0.082

6. Example of an application

In our calculations, we have chosen the 28 Si + 154 Sm system as an example because it involves two quite deformed nuclei. In table 1, we provide the average deformation parameter values $(\bar{\beta}_2, \gamma_0 \text{ and } \bar{\beta}_3)$ as well as the amplitudes of vibration $(b_2 \text{ and } b_3)$ for the quadrupole and octupole modes of these nuclei [2]. Within the GRVM, the nucleus can assume different shapes due to the vibration. We consider that a typical value for the deformation parameter can be obtained from $\beta = \sqrt{\bar{\beta}^2 + b^2}$. Table 1 also provides the β_2 , γ and β_3 values assumed in our calculations for the 28 Si and 154 Sm nuclei.

Before presenting the calculations of potentials, we show the degree of precision of the expansion of the density to second order. The dashed lines in figures 2 and 3 represent the results of (38) for 28 Si and 154 Sm, while the solid lines correspond to the exact results of (9). For the purpose of comparison, also the expansion to first order is presented in the figures through dotted lines. These figures show the matter density as a function of the distance to the origin of the frame of reference, for different spatial directions (θ , ϕ). The laboratory frame of reference was chosen to coincide with the intrinsic frames of $\lambda = 2$ and 3, since all Euler angles were assumed to be zero. Considering that the nuclei are very deformed, the expansion (38) to second order describes the exact density reasonably well. As discussed below, this expansion is precise enough to provide quite accurate results in the calculation of potential strengths.

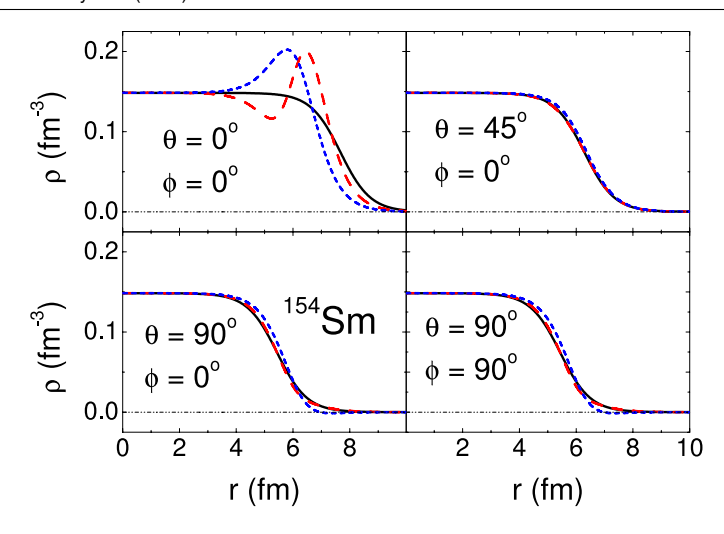


Figure 3. The same as figure 2, but for ¹⁵⁴Sm.

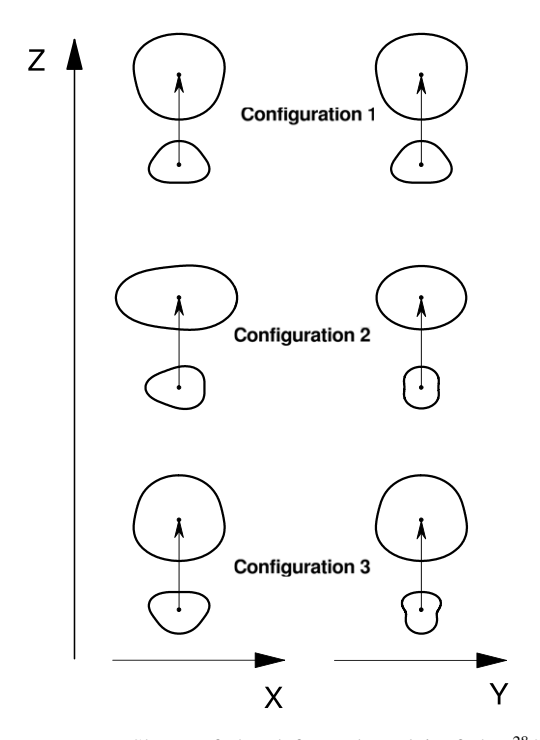


Figure 4. Shape of the deformed nuclei of the 28 Si + 154 Sm system for the three configurations of the Euler angles of table 2. The left side of the figure shows a section of the nuclei in the xz plane, while the right side corresponds to the yz plane. The arrows in the figure represent the separation \vec{R} .

Since we are interested only in studying the precision of the present method to calculate potential strengths, at the moment, we assume without loss of generality that the Z_{Lab} axis is in the direction of \vec{R} . We have considered three different configurations of the Euler angles to calculate the potentials. These configurations differ only by the θ_2 angles, because we set all

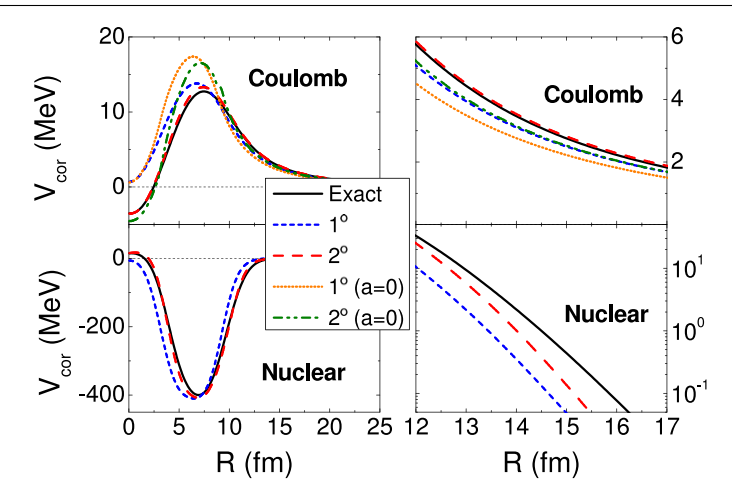


Figure 5. Coulomb (top) and nuclear (bottom) correction potentials for configuration 1 of the 28 Si + 154 Sm system. The lines represent the results of exact (section 3) and approximate (section 5) calculations to first or second order. In the Coulomb case, the approximate calculations were performed with a finite or vanishing value of the nuclear diffuseness. The right side of the figure corresponds to an expansion of the scales in the surface region. In the nuclear case, a logarithmic scale of the modulus of the potential was adopted.

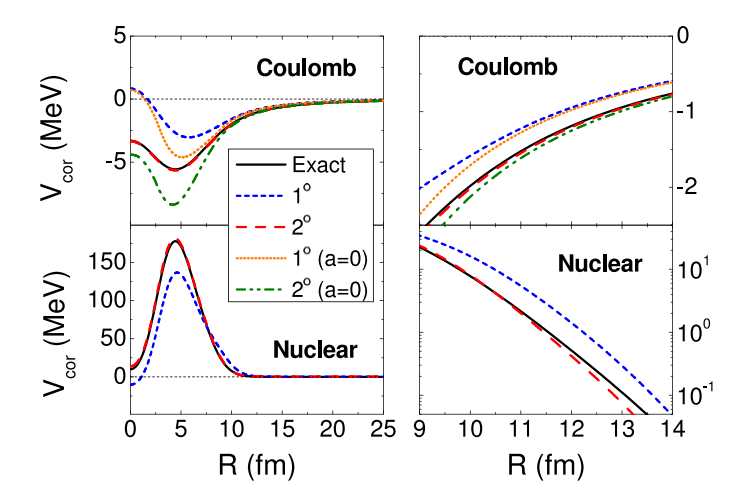


Figure 6. The same as figure 5, but for configuration 2 of table 2.

 $\theta_1 = \theta_3 = 0$. The θ_2 values of $\lambda = 2$ and 3 for both nuclei are presented in table 2. Figure 4 presents an illustration of the shapes of the nuclei for these configurations.

We have performed exact calculations, according to the methods presented in section 2, of the Coulomb and nuclear potentials for the 28 Si + 154 Sm system. We have also calculated the potentials through the method described in section 5, considering the expansion of the densities to first and second orders. In the case of the Coulomb potential, the calculations were performed by assuming both finite and vanishing values for the nuclear diffuseness. The corresponding results for the correction potentials of the three configurations of table 2 are presented in figures 5–7. As expected, the best approximation corresponds to that obtained

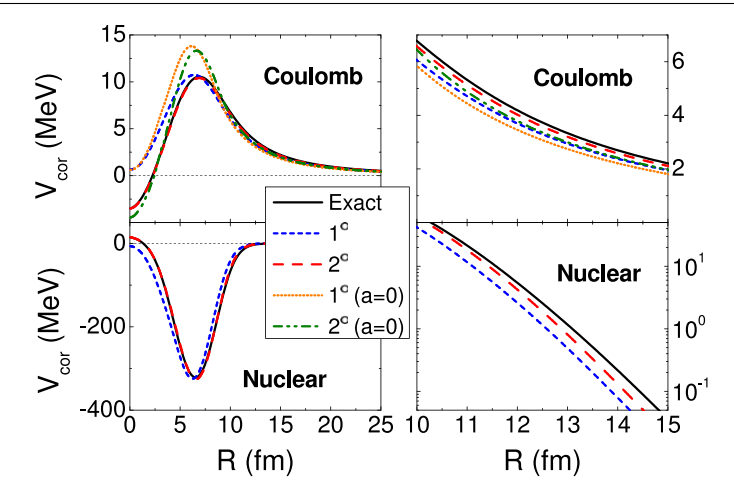


Figure 7. The same as figure 5, but for configuration 3 of table 2.

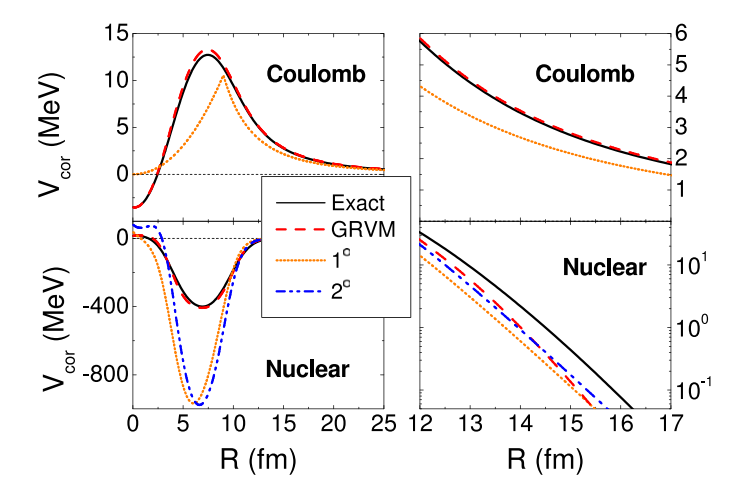


Figure 8. Coulomb (top) and nuclear (bottom) correction potentials for configuration 1 of the 28 Si + 154 Sm system. The solid black lines represent the results of the exact calculations performed as described in section 3. The dashed red lines correspond to the GRVM approximation (section 5), while the others represent the common approximations presented in section 4.

Table 2. The table presents, for each configuration considered in the calculation of the potentials, the values of the θ_2 Euler angles assumed for the quadrupole and octupole modes of ^{28}Si (nucleus 1) and ^{154}Sm (nucleus 2).

Config.			Nucl. 2 $\lambda = 2$	
1	0	0	π	π
2	$\pi/2$	$\pi/2$	$\pi/2$	$\pi/2$
3	π	π	0	0

considering the expansion of the density to second order in the deformations. The value assumed for the nuclear diffuseness clearly has a quite significant effect on the Coulomb potential.

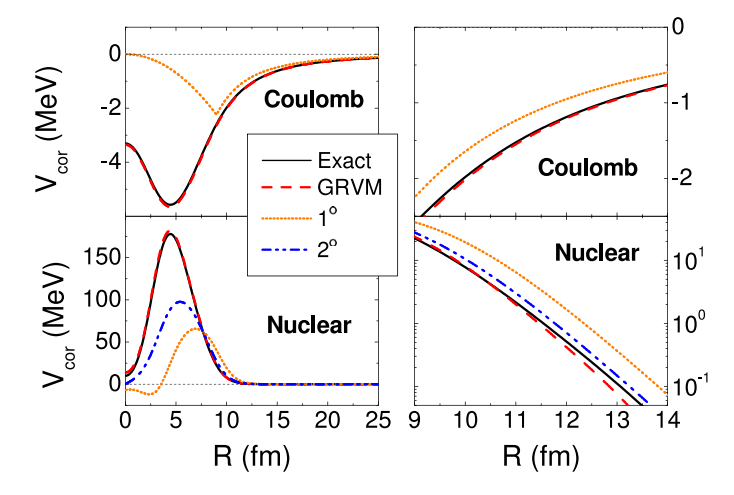


Figure 9. The same as figure 8, but for configuration 2 of table 2.

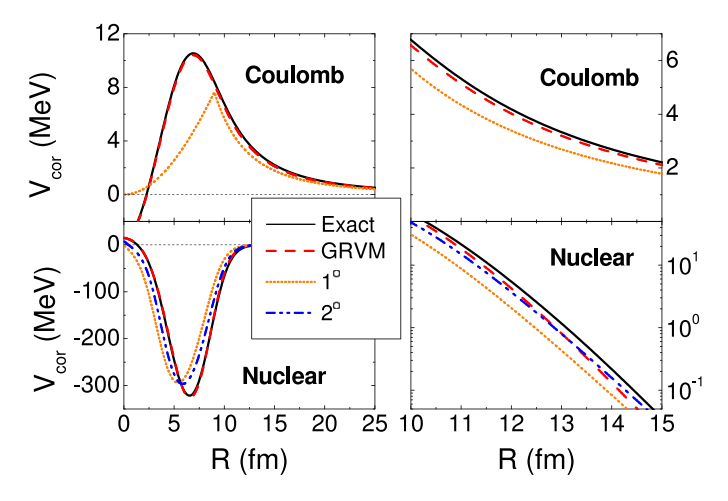


Figure 10. The same as figure 8, but for configuration 3 of table 2.

We denote as the GRVM approximation the method of calculating the potentials according to section 5, with the expansion of the density to second order and assuming the finite value for the diffuseness. We have compared the results of the GRVM approximation with those obtained from the common approximations discussed in section 4. The results for the three configurations of table 2 are presented in figures 8–10. Clearly, the best results are those from the GRVM approach, in particular, with remarkable differences at the inner distances.

7. Conclusion

We have presented a method to calculate double-folding potentials involving deformed densities which is appropriate for future applications in coupled-channel calculations. The present approach is an improvement of the models proposed in [21, 22] to calculate the Coulomb potential, in which the charge distributions were assumed to have a sharp cutoff shape. Within the present model, the results of (18) can be obtained, with quite good accuracy,

through (20), (26), (27), (30) and (42)–(45). In this context, the method is quite general. It can be applied for the set of densities with shape represented by (1) and (2), which includes axially asymmetric distributions, with expansion of Δ to any order of the multipole modes. The interaction $u(\vec{r})$ of (18) can also be quite general (it is required that $\tilde{u}(\vec{k})$ depends only on the modulus of \vec{k}), since our equations are all expressed as functions of its Fourier transform. The model can also be used with different shapes (or deformations and even different interactions $u(\vec{r})$) adopted for the protons and neutrons distributions, since their respective contributions can be calculated separately and then added to obtain the total potential. In this work, we have considered the expansion of the nuclear density only to second order in the deformation parameters. The method can easily be generalized to higher order but this would demand the consideration of more terms in (42).

In the present paper, the method has been developed in the particular context of the GRVM, assuming the Fermi function for the shape of the nuclear distribution and with expansion of the radius up to the octupole mode. Through the comparison of the numerical results obtained in the test case, we verified that the GRVM approach provides much better results than those of common models usually assumed in coupled-channel calculations.

Acknowledgments

This work was partially supported by the Conselho Nacional de Desenvolvimento Científico e Tecnológico (CNPq) and the Coordenação de Aperfeiçoamento de Pessoal de Nível Superior (CAPES).

References

- [1] Eisenberg J M and Greiner W 1970 Nuclear Models (Amsterdam: North-Holland)
- [2] Chamon L C and Carlson B V 2010 Nucl. Phys. A 846 1
- [3] Satchler G R 1983 Direct Nuclear Reactions (Oxford: Clarendon)
- [4] Hagino K and Takigawa N 2012 Prog. Theor. Phys. 128 1061
- [5] Canto L F, Gomes P R S, Donangelo R and Hussein M S 2006 Phys. Rep. 424 1
- [6] Dasgupta M, Hinde D, Rowley N and Stefanini A 1998 Annu. Rev. Nucl. Part. Sci. 48 401
- [7] Balantekin A B and Takigawa N 1998 Rev. Mod. Phys. 70 77
- [8] Reisdorf W 1994 J. Phys. G: Nucl. Part. Phys. 20 1297
- [9] Beckerman M 1985 Phys. Rep. 129 145
- [10] Beckerman M 1983 Rep. Prog. Phys. 51 1047
- [11] Stokstad R G, Eisen Y, Kaplanis S, Pelte D, Smilansky U and Tserruya I 1978 Phys. Rev. Lett. 41 465
- [12] Beckerman M, Salomaa M, Sperduto A, Enge H, Ball J, DiRienzo A, Gazes S, Chen Y, Molitoris J D and Nai-feng M 1980 Phys. Rev. Lett. 45 1472
- [13] Vaz L C and Alexander J M 1981 Phys. Rep. 69 373
- [14] Nobre GPA, Chamon LC, Gasques LR, Carlson BV and Thompson IJ 2007 Phys. Rev. C 75 044606
- [15] Nobre G P A, Silva C P, Chamon L C and Carlson B V 2007 Phys. Rev. C 76 024605
- [16] Nobre G P A and Chamon L C 2007 Phys. Rev. C 76 044608
- [17] Jiang C L et al 2004 Phys. Rev. Lett. 93 012701
- [18] Mukherjee A, Hinde D J, Dasgupta M, Hagino K, Newton J O and Butt R D 2007 Phys. Rev. C 75 044608
- [19] Chamon L C, Nobre G P A and Carlson B V 2009 J. Phys. G: Nucl. Part. Phys. 36 025102
- [20] Satchler G R and Love W G 1979 Phys. Rep. 55 183
- [21] Takigawa N, Rumin T and Ihara N 2000 Phys. Rev. C 61 044607
- [22] Carlson B V, Chamon L C and Gasques L R 2004 Phys. Rev. C 70 057602
- [23] Tamura T 1965 Rev. Mod. Phys. 37 679

- [24] Chamon L C, Carlson B V, Gasques L R, Pereira D, De Conti C, Alvarez M A G, Hussein M S, Candido Ribeiro M A, Rossi E S Jr and Silva C P 2002 *Phys. Rev.* C 66 014610
 [25] Hagino K, Rowley N and Kruppa A T 1999 *Comput. Phys. Commun.* 123 143
- [26] Thompson I J 1988 Comput. Phys. Rep. 7 167
 [27] Raynal J 1981 Phys. Rev. C 23 2571